 doi:10.20944/preprints201803.0095.v1

Article

Improving parametric cyclonic wind fields using recent satellite remote sensing data

Yann Krien [1,*], Gaël Arnaud [1], Raphaël Cécé [1], Jamal Khan [2,3], Ali Bel Madani [4], Didier Bernard [1], A.K.M.S. Islam [3], Fabien Durand [2], Laurent Testut [5], Philippe Palany [4] and Narcisse Zahibo [1]

[1] LARGE, University of the French West Indies, Guadeloupe, France
[2] LEGOS UMR5566/CNRS/CNES/IRD/UPS, France
[3] IWFM, BUET, Dhaka, Bangladesh
[4] Météo France, DIRAG, Martinique, France
[5] LIENSs UMR 7266 CNRS, University of La Rochelle, La Rochelle, France
* Correspondence: ykrien@gmail.com; Tel.: +33 6 16 80 80 51

Abstract: Parametric cyclonic wind fields are widely used worldwide for insurance risk underwriting, coastal planning, or storm surge forecasts. They support high-stakes financial, development, and emergency decisions. Yet, there is still no consensus on the best parametric approach, or relevant guidance to choose among the great variety of published models. The aim of this paper is first and foremost to demonstrate that recent progresses on estimating extreme surface wind speeds from satellite remote sensing now makes it possible to select the best option with greater objectivity. In particular, we show that the Cyclone Global Navigation Satellite System (CYGNSS) mission of NASA is able to capture a substantial part of the tropical cyclones structure, and allows identifying systematic biases in a number of parametric models. Our results also suggest that none of the traditional empirical approaches can be considered as the best option in all cases. Rather, the choice of a parametric model depends on several criteria such as cyclone intensity and/or availability of wind radii information. The benefit of our approach is demonstrated by comparing traditional models with an improved vortex for hurricane Maria in the Caribbean. The wave heights computed by a wave-current hydrodynamic coupled model are found to be much better reproduced, with a significant reduction of the model biases. The results and approach presented in this study should shed new light on how to handle parametric cyclonic wind models. This will help the scientific community to conduct better wind, waves and surge analysis for tropical cyclones.

Keywords: Remote sensing; cyclones; parametric models; hurricanes; CYGNSS; ASCAT; storm surges; waves; winds

1. Introduction

Since the overview of Vickery et al. [1], numerical atmospheric models have been increasingly applied in storm surge prediction or coastal hazard assessment studies [2-5]. Nonetheless, parametric models deriving cyclonic wind fields from a few input parameters (pressure drop, maximum velocity, wind radii, location of the cyclone center, etc) are still widely used by the research and insurance communities, due to their simplicity, efficiency, and low-computational costs [6-12]. This is especially true for studies investigating storm surge hazards with statistical approaches, which require the construction of a large number of synthetic storms [13-16].

For a few decades (and still often today) the parametric surface winds were simply derived as the sum of an axisymmetric wind field and a uniform vector to mimic the asymmetry due to the storm translation speed. Vivid debates arose to determine the best way to estimate both components, which is a particularly relevant issue since large discrepancies of the synthesized wind field occur

depending on the chosen method [17]. This kind of approach where the tropical cyclone (TC) size is generally determined by a single parameter (the radius of maximum winds), presents several drawbacks. In particular, it generally does not satisfactorily represent the TC wind asymmetry, which can be due to many factors such as blocking action by a neighbor anticyclone, boundary layer friction, or terrestrial effects [18].

To date, the increasing availability of satellite remote sensing data makes it possible to better depict and forecast the wind structure of TCs and its variations with azimuth. Whether they are based on infrared imagery and data [19-21], scatterometry [22-23], X-band, C-band and L-band radiometry [24-29], or global navigation satellite system-reflectometry (GNSS-R) [30-32], all these data can provide information about the 34-kt, 50-kt, and/or 64-kt wind radii in each TC quadrant. These radii are now commonly reported in advisories issued by warning centers.

Yet, to our knowledge, only very few studies investigating TC winds, cyclonic-induced waves, or storm surges through parametric models account for all this information, whether for forecasts or hindcasts. Besides, it is striking to see that even now, there is neither consensus nor even real debate on the best gradient wind model, i.e. the parametric model that will represent with the greatest accuracy the increase and decay of wind speed as a function of distance to the TC center. A vivid example of this is the Holland [33] vortex. Although known to present significant drawbacks [34], this model is still widely used by the research and insurance communities all over the globe. Other commonly used parametric wind models (for which there is room for improvement) include for example Jelesnianski and Taylor [35], or Emanuel and Rotunno [36]. New models are proposed almost every year [18,37], but the published studies also generally suffer from one or several drawbacks, including:

- a *lack of information about the parameters considered*. For example, the empirical surface wind reduction factor (SWRF [38]) used for computations is rarely indicated, although it is thought to play a significant role in the estimated surface wind speeds [17].
- *comparisons/validations with a limited number of observed data*. In-situ observations of surface wind speed are relatively sparse for TCs, as they spend most of their lifetime over the oceans, where the density of buoys able to record extreme winds is relatively small. Besides, the wind recorded by meteorological stations is often biased because of terrestrial effects, which makes it difficult to compare observations with parametric values in a consistent way. Although these issues are offset to some extent in the North Atlantic and East Pacific thanks to aircraft reconnaissance, it remains a major problem in all oceanic basins.
- *comparisons/validations with a limited number of parametric wind models*. Except the work of Lin and Chavas [17], we are not aware of any study investigating parametric wind models over a wide range of parameters and methods. New proposed models are often compared to the Holland [33] or Jelesnianski and Taylor [35] approaches to assess their quality, and disregard more recent models such as Willoughby et al. [39] or Emanuel and Rotunno [36].
- *comparisons/validations with parametric models which do not include all the available information about the TC wind structure.* As noted before, very few studies take into account all the available information about wind structure, such as the 34-kt, 50-kt, and 64-kt wind radii for each quadrant. Most of the time, only the hurricane-force (i.e. 64kt) wind radii are used, which potentially results in errors far from the cyclone center.

Yet, indirect surface wind speed measurements using remote sensing data are now expected to be mature enough to help us overcome most of these limitations. The recent availability of data from CYGNSS (Cyclone Global Navigation Satellite System), a spatial mission dedicated to wind speeds retrieval near the eye of TCs, is a promising example.

The main objectives of this paper are twofold : 1-to investigate the benefits of using recent datasets of satellite remote sensing data such as CYGNSS or ASCAT (Advanced Scatterometer) to get

information on TCs structure, 2- to determine how this information can be used to identify a relevant parametric model.

After a short description of data and wind models used in the present study (section 2), we compare CYGNSS and ASCAT data with parametric models constrained by observations for 16 recent hurricanes (section 3). The aim is to provide a first evaluation of the usefulness of these remote sensing data as proxy for surface wind speeds. As we will show, our results suggest that CYGNSS and ASCAT data provide indeed reliable estimates for extreme and moderate wind speeds respectively. We then hypothesize that it is indeed the case, and study several parametric models in greater details to assess their capability to reproduce the findings of the past studies (section 4). We then perform numerical hindcasts of hurricane Maria (2017) using several parametric formulas, and compare significant wave heights computed with real in-situ data (section 5). The aim is to further test the validity of our approach, and to assess its benefits for improving cyclonic wind fields. We finally briefly review the main findings of the manuscript and give concluding remarks (section 6).

2. Data and Methods

2.1. Cyclone selection

With six major hurricanes, two of which reaching the category 5, 2017 was an extremely active season for cyclones in Atlantic. Thanks to aircraft reconnaissance, large quantities of high-quality in-situ data were collected and incorporated into models to better reproduce the hurricanes and their evolution for a wide range of intensities and sizes. Besides, the CYGNSS mission of NASA (dedicated to surface wind speed measurements in extreme conditions) was launched just in time to collect data for this season. These conditions are ideal for revisiting the structure of TCs, and the ability of parametric models to approximate it. In this study, we considered most of the hurricanes that occurred both in Atlantic and East Pacific during the 2017 season. In all, 16 events were taken into account (Table 1).

Table 1. List and characteristics of the 16 hurricanes considered in this study. The radii at 34-kt, 50-kt, and 64-kts (r34, r50, and r64 respectively) are given in nautical miles.

Number	Name	Basin	Dates	Maximum Category	Min/max r34 at the maximum	Min/max r50 at the maximum	Min/max r64 at the maximum
1	Dora	Pac.	25/06 → 28/06	1 (80kt)	40/70	20/40	15/25
2	Eugene	Pac.	07/07 → 10/07	3 (100kt)	60/110	40/80	20/30
3	Franklin	Atl.	07/08 → 10/08	1 (75kt)	60/130	30/50	NA/30
4	Gert	Atl.	13/08 → 17/08	2 (90kt)	50/120	15/60	NA/30

5	Harvey	Atl.	17/08 → 30/08	4 (115kt)	70/120	40/60	20/35
6	Hilary	Pac.	24/08 → 30/08	2 (90kt)	60/90	30/50	15/20
7	Irma	Atl.	30/08 → 11/09	5 (160kt)	80/160	50/100	30/45
8	Irwin	Pac.	23/07 → 01/08	1 (80kt)	30/60	10/30	NA/15
9	Jose	Atl.	05/09 → 22/09	4 (135kt)	50/120	30/50	20/30
10	Katia	Atl.	06/09 → 09/09	2 (90kt)	60/60	20/40	15/20
11	Kenneth	Pac.	19/08 → 23/08	4 (115kt)	60/90	30/50	15/25
12	Lee	Atl.	16/09 → 30/09	3 (100kt)	60/80	40/50	25/30
13	Maria	Atl.	16/09 → 30/09	5 (150kt)	100/150	60/80	35/50
14	Max	Pac.	13/09 → 15/09	1 (70kt)	30/40	20/20	10/10
15	Norma	Pac.	14/09 → 19/09	1 (65kt)	70/80	30/50	NA/25
16	Otis	Pac.	16/09 → 19/09	3 (100kt)	40/60	20/40	10/20

For each of these events, we considered the following data provided by the NHC (National Hurricane Center) advisories: location of the cyclone center, minimum pressure, maximum wind speed, radii of the 34-, 50-, and 64-knot winds in the four quadrants at every 6 hours. Most of these data were calibrated using aircraft reconnaissance and are consequently considered reliable.

2.2. Remote sensing data

We also collected the full dataset distributed by the CYGNSS and ASCAT science team members for the 2017 hurricane season in Atlantic and East Pacific.

The CYGNSS mission [31] consists of a eight satellites-constellation in low-inclination circular orbit that receive direct and reflected GPS L1 (1.575 Ghz) signals to infer surface wind speeds and sea roughness, even for intense rainfalls typically observed during hurricanes. It allows for a good spatial and temporal coverage, with mean and median revisit times over the tropics of 7.2h and 2.8h respectively [32]. The 25km- resolution data considered here (v2.0) have been validated and calibrated using cyclones of the 2017 season, including most of the events considered in this study (Table 1). We tested here several Level 2-wind speed products proposed by the CYGNSS team:

- The "wind speed" (*ws*) product is derived from the best fit to both the normalized bistatic radar cross-section (NBRCS) and leading edge slope (LES) of the integrated delay waveform given by the delay-Doppler maps (DDM [40]), using a fully developed seas geophysical model function (GMF);
- The "yslf_les_wind_speed" (*les*) wind product is derived from only the LES of the DDM, using a young seas / limited-fetch GMF;
- The "yslf_nbrcs_wind_speed" (*nbrc*) product is derived from only the NBRCS, using the young seas / limited-fetch GMF.

ASCAT [22,41] consists of C-band scatterometers mounted on the satellites MetOp-A and MetOp-B, that were launched in 2006 and 2012 respectively. The emitting antennas transmit pulses at 5.255 GHz and extend on either side of the instrument, which results in a double 500km-wide swath of observations. We use here the 25km-resolution coastal product, which give more wind data close to the coast [42].

2.3. Parametric wind models

For a given cyclone and parametric gradient wind profile, we estimated the surface wind speed associated to each CYGNSS and ASCAT data point according to the following main steps:

1- From the NHC advisories, we estimated the surface background wind relative to the cyclone translation velocity at the time of acquisition of the considered CYGNSS/ASCAT data point. Following the approach of Lin and Chavas [17], we assumed that this wind is decelerated by a factor α=0.56 and rotated counter-clockwise by an angle β=19.2° from the free tropospheric wind.

2-We removed the translational portion of the wind speed from the maximum observed wind velocity and the 34-, 50-, and 64kt winds.

3-We converted surface velocities to velocities on top of the atmospheric boundary layer by applying an empirical surface wind reduction factor SWRF [38]. In the following sections, we specified SWRF=0.9. Other values were tested, but for the sake of simplicity results are not presented here (they add very little to the conclusions of this paper).

4-We estimated the maximum wind radii for the four quadrants, using the chosen parametric gradient wind profile, and the available wind radii information. For each quadrant, up to three radii of maximum wind are thus obtained: one from the 64-kt wind radius (R_{m64}), another from the 50-kt wind radius (R_{m50}), and a last one from the 34-kt wind radius (R_{m34}).

5-Depending on the available wind radii information considered, we computed R_{m64}, R_{m34} or all the radii of maximum winds (R_{m64}, R_{m50}, and R_{m34}) for the data point azimuth, using a spline interpolation.

6-We computed the wind speed values at the CYGNSS/ASCAT data point obtained using the chosen parametric gradient wind profile and the radii of maximum winds considered (R_{m64}, R_{m34}, or all three of them).

7-We assessed the wind speed at the CYGNSS/ASCAT data point, using a weighted average of the wind speeds obtained in the previous step. We followed the procedure proposed by Hu et al. [43], which ensures that all the wind radii information is satisfied.

8-We obtained the surface wind speed by multiplying the result by SWRF.

9-The wind speed obtained in the previous step was combined with the surface background wind computed in step 1 to get the final parametric wind speed at the CYGNSS/ASCAT data point considered.

This procedure is repeated for all the storms, gradient wind profiles, and CYGNSS/ASCAT Level 2-data points within a distance of 200km from the cyclone center. The parametric models considered here are given in Table 2.

Table 2. Parametric wind models considered in this study. For all of them, an empirical surface wind reduction factor [38] SWRF=0.9 was prescribed. Comparisons are only made for data within a distance of 200km from the cyclone center. The translation vector is reduced by a factor α=0.56 and rotated counter-clockwise by an angle β=19.2°, according to the findings of Lin and Chavas [17]. Here, V_m and R_m are the maximum wind speed and the radius of maximum winds. r refers to the distance to the TC center, and f to the coriolis coefficient.

Name	Main reference	Formula
E11	*Emanuel and Rotunno [36]*	$V(r) = \frac{2r(R_m V_m + 0.5 f R_m^2)}{R_m^2 + r^2} - \frac{fr}{2}$
E04	*Emanuel [44]*	$V(r) = V_m \frac{R_{0-r}}{R_0 - R_m} \left(\frac{r}{R_m}\right)^m \left(\frac{(1+b)(n+m)}{n + m\left(\frac{r}{R_m}\right)^{2(n+m)}} + \frac{b(1+2m)}{1+2m\left(\frac{r}{R_m}\right)^{2m+1}} \right)^{0.5}$ with b=0.25, m=1.6, n=0.9, R_0=420km
J92	*Jelesnianski et al [45]*	$V(r) = \frac{2rR_m V_m}{R_m^2 + r^2}$
H80	*Holland [33]*	$V(r) = \sqrt{\left(\frac{R_m}{r}\right)^B \frac{B\Delta P exp\left(-\left(\frac{R_m}{r}\right)^B\right)}{\rho} + \frac{r^2 f^2}{4}} - \frac{fr}{2}$ with $B = \frac{V_m^2 e\rho + f V_m R_m e\rho}{\Delta P}$, $\rho = 1.15$, $e = \exp(1)$
H80c	*Holland [33] with cyclostrophic*	$V(r) = \sqrt{\left(\frac{R_m}{r}\right)^B \frac{B\Delta P exp\left(-\left(\frac{R_m}{r}\right)^B\right)}{\rho}}$

	approximation	with $B = \frac{V_m^2 e\rho}{\Delta P}$, $\rho = 1.15$, $e = \exp(1)$
M16	*Murty et al. [37]*	$V(r) = V_m \left(\frac{2rR_m}{(R_m^2 + r^2)}\right)^n$ with $n = 3/5$
W06	*Willoughby et al. [39]*	For $0 \le r \le R_m$: $V(r) = V_m \left(\frac{r}{R_m}\right)^n$ with $n = 0.79$ For $r \ge R_m$: $V(r) = V_m exp\left(-\frac{r - R_m}{X}\right)$ with $X = 243km$

3. Comparison of CYGNSS and ASCAT data

The biases between the remote sensing data and the mean (i.e. averaged over all empirical models) parametric winds are displayed in Figure 1 for different cyclone categories and distances to the center. Computations were performed only when more than 30 data points were available for a given intensity/distance class. In practice, the comparison was possible for almost all cases, as hundreds or even thousands of space-borne observations were available for each class.

Parametric models have been constrained by all the information provided by the NHC in the advisories, to ensure that they give the best approximation to real winds. Small biases (in absolute terms) suggest that remote sensing data and parametric winds are consistent, so that they both give satisfactory results a priori. Indeed, since satellite data and empirical formulas were calibrated independently, it would be surprising to achieve good matches because of similar systematic errors. Large biases indicate on the contrary that remote sensing data and/or parametric winds overestimate or underestimate the real winds.

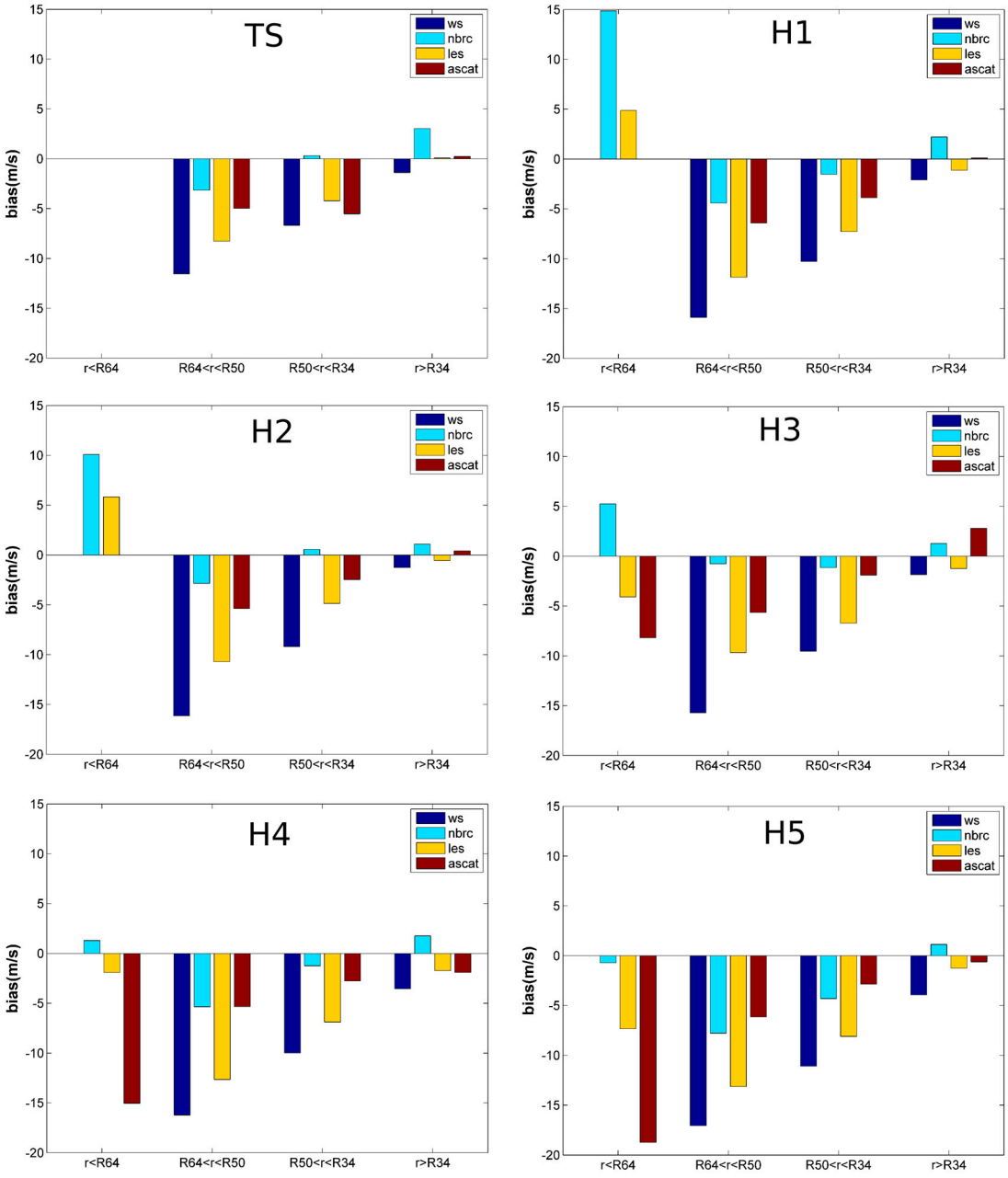

Figure 1. Bias between the remote sensing data and the parametric winds averaged over all empirical models (negative/positive values indicate that remote sensing data are negatively/positively biased compared to the mean parametric winds) . Different categories of distance to the cyclone center (r) and cyclone intensities are considered. TS stands for tropical storms, H1, H2, H3, H4, and H5 to the cyclone category (1, 2, 3, 4, and 5 respectively). R34, R50, and R64 are the radii for the 34-kt, 50-kt, and 64-kt winds. *ws*, *nbrc*, and *les* are three different CYGNSS products (see section 2).

Regarding ASCAT data, Figure 1 shows that the absolute value of bias is low (less than about 2-3m/s) for radius larger than R34, but increases with cyclone category and decreasing distance to the cyclone center, up to almost 20m/s. These results suggest that ASCAT data are a good proxy for wind speeds lower than 34-kt, but that they poorly represent stronger winds. Since the bias is negative in that case, extreme winds are found to be underestimated by ASCAT, which is consistent with previous published papers [46]. These first results hence provide a certain level of confidence in our parametric models.

231 The "wind speed" (*ws*) product is found to give systematically more negative biases than
232 ASCAT, and thus probably often underestimates the velocities (Figure 1). However, the absolute
233 value of bias remains relatively low for radius larger than R34, which suggests that this product
234 might be a good proxy for moderate and (potentially even more) low wind speeds. As this product
235 was developed for fully developed seas, these results were also expected.
236 Wind speeds derived from only the LES of the DDM ("*les*" in Figure 1) display, again, negative
237 biases for r>R64. However, those remain smaller in absolute value compared to "*ws*", which makes
238 sense since this product has been derived using a young seas / limited-fetch GMF that is expected to
239 be more suitable for our test cases. Considering the potential errors on parametric models, it could
240 be a proxy as good as ASCAT for radius larger than R34. Above all, this product shows significantly
241 reduced biases for r<R64. This suggests that it yields better estimates of surface wind speeds than
242 ASCAT close to the eyewall.
243 The wind speeds derived from only the NBRCS ("*nbrc*" in Figure 1) outperform the other
244 products in most cases for radius lower than R34, with bias generally lower than 5m/s in absolute
245 value. The main exception is the wind for radius lower than R64 for minor cyclones (category 1 or 2),
246 where the bias reaches 10 to 15m/s. One plausible explanation is that the resolution of CYGNSS
247 (25km) is too low to capture the surface wind speeds in these area, especially for weak cyclones
248 where the 64kt radii are very close to the eyewall, i.e. to places where wind speeds vary quickly as a
249 function of distance to the center. This problem is presumably less severe for major cyclones
250 (category 3 or more) because of a larger extent of hurricane-force winds (Table 1).
251 Based on these findings, we will hypothesize in the following section that the ASCAT and
252 CYGNSS/NBRC products are the best surface wind speeds proxy for r> R34 and r<R34 respectively.
253 We will check in sections 4 and 5 whether this assumption gives results consistent with previous
254 work and in-situ data, to confirm (or invalidate) the hypothesis a posteriori. It is noteworthy to
255 mention that no estimation will be made for radius lower than R64 in the case of weak (category 1-2)
256 cyclones, as none of the space-borne products tested here is expected to be really reliable in these
257 cases.

258 **4. Performance of parametric wind models**

259 The biases between the various parametric models and the estimated surface wind speeds are
260 plotted in Figure 2 as a function of storm intensity, distance to the cyclone center, and calibration
261 method (using only radii at 34kt, only radii at 64kt, and all radii information for the left, middle and
262 right panels respectively). The color bar shows the absolute value of bias. Blue colors correspond to
263 small biases (in absolute value), and thus suggest that the parametric model should work well for
264 the intensity/distance class considered. Conversely, red colors indicate that the model is expected to
265 perform poorly.

 doi:10.20944/preprints201803.0095.v1

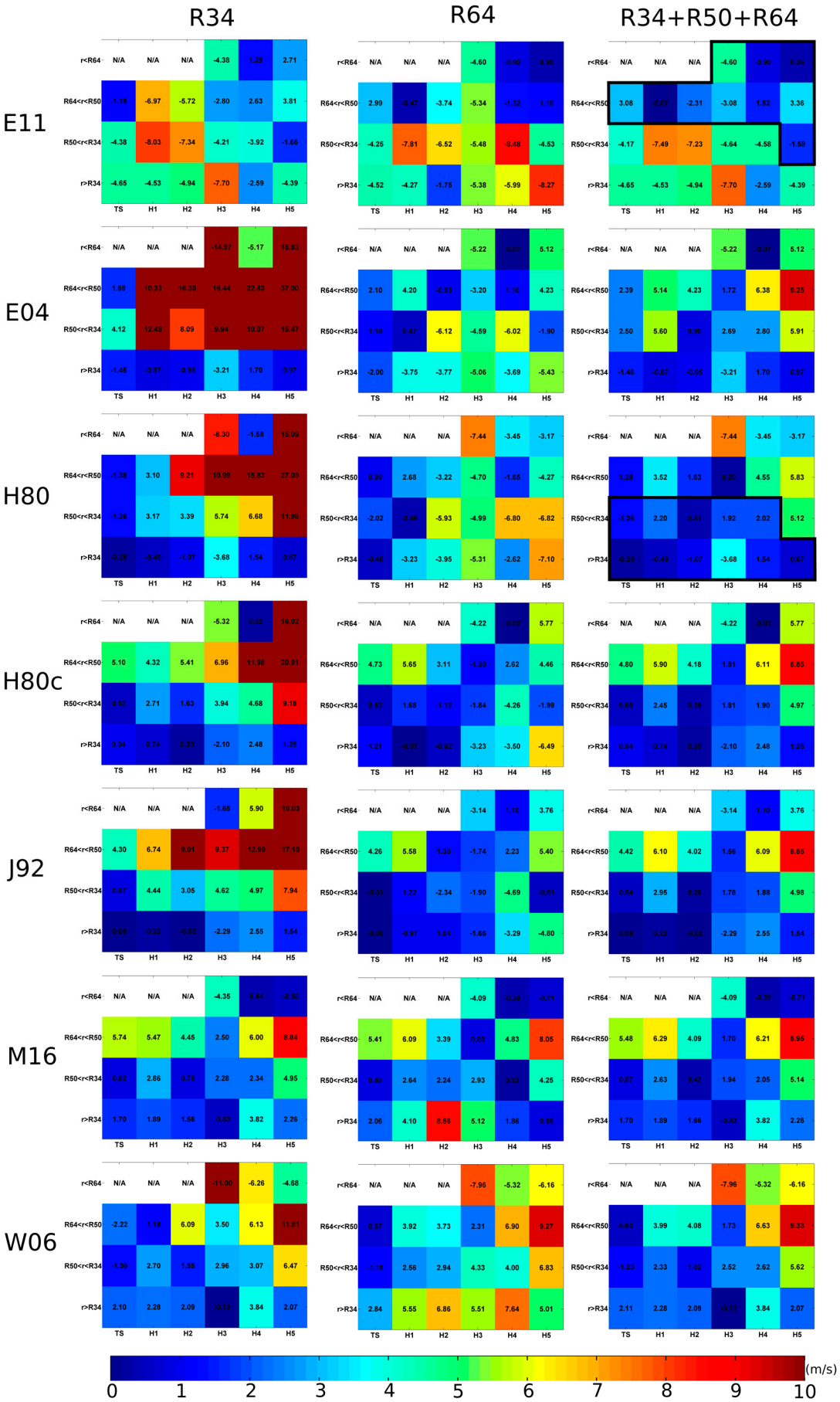

Figure 2. Diagrams displaying the bias between the different parametric models and the estimated surface wind speeds for all the events considered here, as a function of storm intensity and distance to the cyclone center (x- and y-axis respectively for each diagram), as well as calibration method (using only radii at 34kt, only radii at 64kt, and all radii information for the left, middle and right panels respectively). The color bar (the same for all diagrams) shows the absolute value bias. The values are displayed for each category/distance cell. The black contours indicate the category/distance classes for which we consider E11 and H80 models in section 5 (model E11H80).

The results are found to be consistent with most of the previous works. For instance:

- The inner region solution of Emanuel and Rotunno [36], E11, generally gives the smaller bias (hence the best results) close to the storm center (typically, for r<R50), especially for intense and well defined cyclones. Conversely, it is found to underestimate significantly the wind speeds far from the center, even when prescribing the radii at 34-kt. E04 performs much better for the outer region, but poorly near the center. E11 and E04 can thus be merged to develop a complete TC radial wind structure as proposed by Chavas et al. [47];
- When solely constrained by radii close to the cyclone center (here R64), the Holland profile (H80) tends to underestimate the winds in the outer region, as noted by Willoughby and Rahn [34]. It can also lead to broad wind maximum, and thus wind overestimations a few dozens of kilometers from the center for strong cyclones (typically, for R64<r<R50, as can be seen in the right and left panels for example, or in Willoughby and Rahn [34])
- J92 tends to overestimate the wind speeds by a few m/s, as suggested by Lin and Chavas [17];
- The results are generally much better when considering a family of profiles with two characteristic lengths, as proposed by Willoughby et al [39]. For example, the performance of the Holland model H80 is increased when both radii at 34-kt and 64-kt are prescribed;
- Models such as W06 or M16 (which decay exponentially or as a power-law outside the eye) perform well if the 34-kt radii are prescribed properly, which is consistent with the findings of Willoughby et al. [39] and Murty et al. [37].

These findings support again our hypothesis that the ASCAT and CYGNSS/NBRC products are relatively good proxies for surface wind speeds, for r> R_{34} and r<R_{34} respectively. To further increase confidence, we performed numerical hindcasts of hurricane Maria (2017) based on a hydrodynamic model forced by winds generated using various parametric formulas. We then compared significant wave heights computed with real in-situ data (section 5).

5. Comparison with in-situ data

Hurricane Maria was the deadliest storm of the 2017 Atlantic season. Recorded as a category 5 event, it caused catastrophic damages in Dominica and Puerto Rico, as well as widespread flooding and crop destructions in Guadeloupe. We tested here the ability of several parametric models to properly represent the wind pattern evolution during Maria by comparing the significant wave heights observed at buoys in the Lesser Antilles with those computed using a wave-current coupled model forced by a sub-set of the various parametric winds considered in the previous section. The model is based on the code SCHISM-WWM [48]. The computational domain is represented in Figure 3. Resolution spans from 10km far from the region of interest (where the bathymetry is derived from GEBCO), up to about 100m in Guadeloupe and Martinique where we have the best bathymetric data (ship-based soundings from the SHOM, the French Naval Hydrographic and Oceanographic Department). The model is forced by:

- astronomic tidal potential over the whole domain (12 constituents);
- 26 tidal harmonic constituents at the open boundaries, provided by the global FES2012 model [49] ;
- parametric pressure fields [33];

- parametric winds blended with CFSR (Climate Forecast System Reanalysis [50]) wind data. The parametric winds are prescribed for radii less than R_{34}, whereas CFSR data are imposed for r > 1.5 R_{34}. In between, a smooth transition is ensured using a weighing coefficient varying with the radius r.

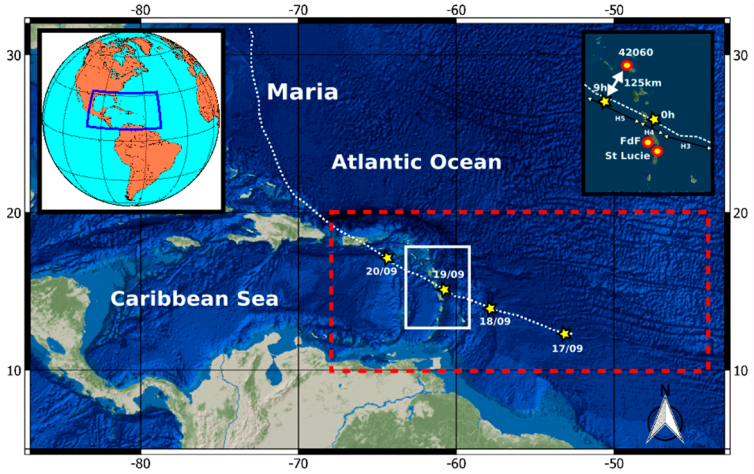

Figure 3. Study area. The computational domain is depicted with the dashed red contour. The dashed white line represents the track of hurricane Maria. The location of the buoys used for comparison is given in the upper-right corner box.

We considered here five parametric models: E11 and H80, constrained using either the 64-kt wind radii only, or all the wind radii information, and E11H80, for which we chose to blend the wind speeds inferred from E11 for the inner core region with those given by H80 for the outer region (see the black contours in Figure 2). E11H80 was chosen to test the benefit of using the results of previous section to improve parametric wind fields. It is noteworthy to mention that we did not try here to build the best model possible. Indeed, the main aim was just to see if better results could be obtained when using a combination of models that should reduce the biases, according to Figure 2.

The reader is referred to Krien et al [9] for greater details about the model and the numerical strategy.

We compared the significant wave heights (Hs) computed by the model with the Hs recorded by three buoys located in the Lesser Antilles (Figure 3): Fort de France (FdF) and Sainte Lucie, owned by Meteo France, as well as 42060, maintained by the National Data Buoy Center (NDBC). The latter went adrift during the peak of Maria, hence the decrease of Hs was unfortunately not captured.

Table 3. Bias, root mean square error (RMS) and normalized RMS (NRMS) obtained when comparing numerical simulations with in-situ significant wave heights.

		42060	Fort de France	St Lucie
H80 (R64)	Bias	0.1m	-0.85m	-0.43m
	RMS	1.2m	0.9m	0.55m
	NRMS	27.1%	41.8%	24%
H80 (All)	Bias	1.5m	0.9m	0.64m
	RMS	2m	1.06m	0.84m

	NRMS	46%	49.3%	36.6%
E11 (R64)	Bias	-1.4m	-0.8m	-0.44m
	RMS	1.5m	0.87m	0.56m
	NRMS	35%	40.3%	24.5%
E11 (All)	Bias	-0.9m	-0.21m	-0.19m
	RMS	0.9m	0.34m	0.43m
	NRMS	21.3%	15.8%	18.7%
E11H80 (All)	Bias	-0.7m	0.01m	-0.04m
	RMS	0.7m	0.31m	0.44m
	NRMS	17.4%	14.5%	19.2%

Results (Table3, Figure 4) show that:

- H80 and E11 constrained only by the 64-kt wind radii (R64) give the worst results, with Hs generally significantly underestimated, and NRMS ranging between 20% and 50% (Table 3).
- Trying to improve these models by constraining all the 34-kt, 50-kt, and 64-kt wind radii (All) results in much better performance for E11, with reduced bias and NRMS (15 to 22% approximately). This suggests that E11 satisfactorily represents the TC structure, at least as long as the hurricane (here in category 4-5) remains relatively close to the buoys. It tends to underestimate Hs (in Sainte Lucie for example) when the storm moves further away.
- On the contrary, the H80 model strongly overestimate Hs as long as the storm remains close to the buoys, but the prediction is better when Maria moves further away. This is again consistent with the results of Figure 2.
- The best results are obtained here for the model E11H80. The bias is found to be considerably reduced compared to E11constrained with all wind radii.

These results are consistent with those presented in Figure 2 (keeping in mind that Maria is here a category 4-5 hurricane, and that it passes relatively close to the buoys, see Figure 3), and the conclusions of section 4. This further increases our confidence in the approach presented here, and suggests that Figure 2 could be used as a preliminary step to select one model instead of another, depending on the case study.

 doi:10.20944/preprints201803.0095.v1

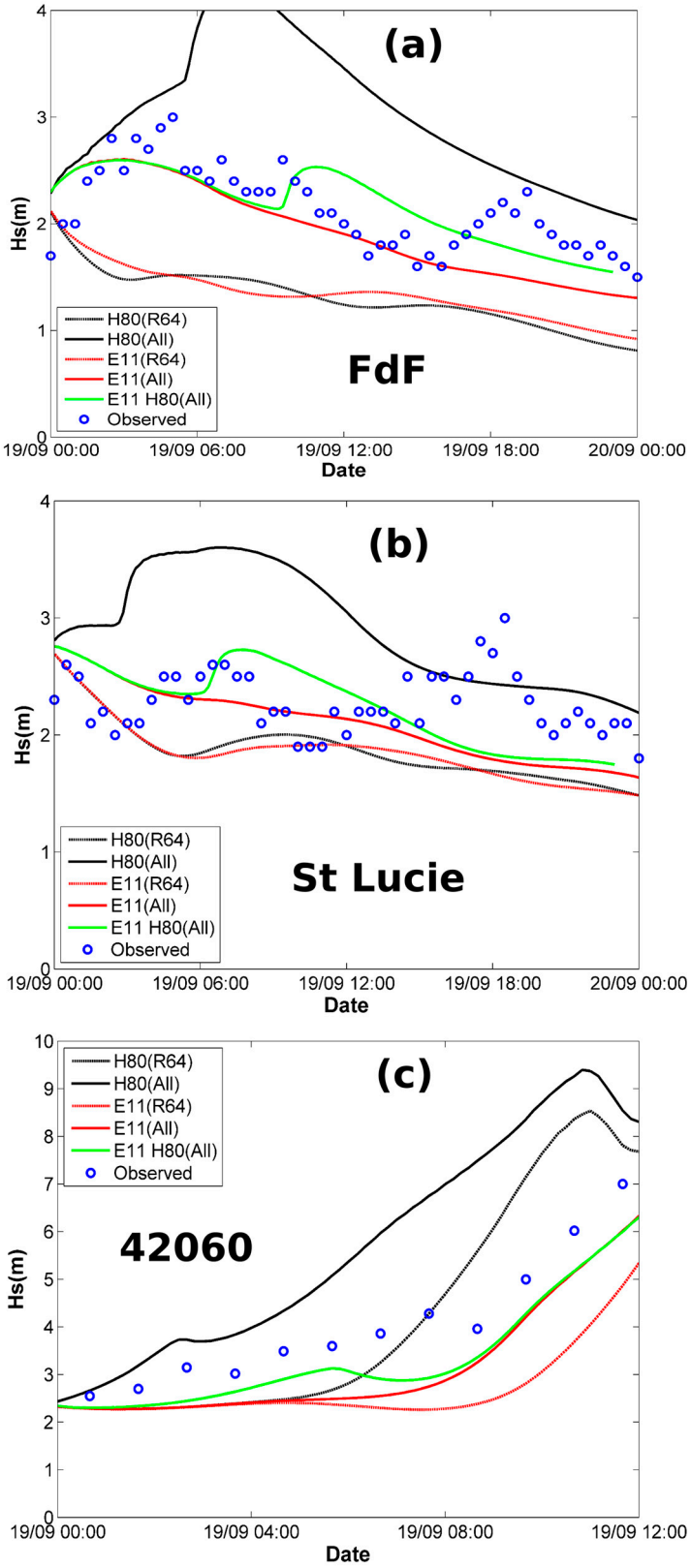

Figure 4- Significant wave height time series for different parametric models. "R64" denotes a model constrained only by the 64-kt wind radii. "ALL" indicates a model constrained with all the available information (34-kt, 50-kt, and 64-kt wind radii). E11H80 corresponds to a blend of the model E11 (for the inner core region) and H80 (for the outer region). Results for Fort-de-France, Sainte-Lucie, and the 42060 station are displayed in (a), (b), and (c) respectively.

6. Conclusions

Taking advantage of an extremely active 2017 hurricane season in the tropical Atlantic Ocean and the Eastern Pacific soon after the launch of the CYGNSS mission, we revisited some of the main parametric wind models used for storm surge hazard assessment or prediction of cyclonic waves, and investigated the potential of recent remote sensing data to estimate surface wind speeds under extreme conditions. Using an innovative approach, we first confirmed the findings of a number of previous studies: the inability of ASCAT data to reproduce strong winds for instance [51], or systematic bias in several parametric models, as stated by Willoughby et al. [39], Lin and Chavas [17] or Chavas et al. [47]. All these results are displayed in a "user-friendly" figure (Figure 2) that should be helpful for the readers to identify the model most suited for their case study.

We emphasize that our main aim here is not to encourage using or discarding a specific parametric model, and even less to propose a new one. First, because we did not test all the published models. Second, because each author uses a specific combination of parameters and approach to mimic the wind field, so that it would be presumptuous to draw definitive conclusions. The main finding of this paper is thus the following: satellite remote sensing is now mature enough to provide relevant information about the performance of parametric cyclonic wind models, even if further work is needed, especially to access to the full structure of TCs close to the eyewall. We focused here mainly on the CYGNSS mission, but there is little doubt that other type of data (such as ASCAT for example) can also be valuable. Remote sensing has now become a powerful tool that should be used to validate or improve existing parametric approaches, in order to conduct better wind, waves, and surge analysis for TCs.

It is noteworthy to conclude by mentioning that even with the improved model tested here for Maria (see section 5), the NRMS remains relatively high (15-20%). Indeed, the temporal resolution (6-hours) is not sufficient to allow parametric models to reproduce the short-term variations of track, translation speed, or wind asymmetry. This stresses the need for higher temporal sampling of data (location of the cyclone center, maximum wind speed, wind radii, etc), and greater efforts to improve the efficiency of numerical atmospheric models.

Acknowledgments: This study was founded by the ERDF/C3AF project as well as the IRD. Our warm thanks to the CYGNSS and ASCAT science team members for their work. ASCAT and CYGNSS data were provided by the KNMI and PODAAC data center respectively. Data at Fort-de-France and Sainte-Lucie were made available by the CEREMA (CANDHIS database).The significant wave heights at station 42060 were provided by NDBC.

Author Contributions: Yann Krien conceived the idea and wrote most of the paper; Gaël Arnaud, Raphaël Cécé and Jamal Khan contributed to the development of the analysis tools; Gaël Arnaud, Ali Bel Madani and A.K.M.S. Islam arranged the figures and corrected a number of errors in the first version of the manuscript. Didier Bernard, Philippe Palany and Narcisse Zahibo prepared the project C3AF which funded about 66% of the work presented here. Fabien Durand, Laurent Testut and A.K.M.S. Islam played a major role for obtaining the IRD grant (about one third of total fundings). The manuscript also greatly benefited from their proofreading and suggestions.

Conflicts of Interest: The authors declare no conflict of interest.

References

1. Vickery, P. J., Masters, F.J., Powell, M.D., Wadhera, D. Hurricane hazard modeling: The past, present, and future, *J. Wind Eng. Ind. Aerodyn*. **2009**, 97, 392–405, doi:10.1016/j.jweia.2009.05.005.
2. Lin, N., Smith, J.A., Villarini, G., Marchok, T.P., Baeck, M.L. Modeling extreme rainfall, winds, and surge from Hurricane Isabel (2003), *Weather Forecast*. **2010**, 25, 1342–1361, doi:10.1175/2010WAF2222349.1.
3. Hsiao, L. F., Chen, D.S., Kuo, Y.H., Guo, Y.R., Yeh, T.C., Hong, J.S., Fong, C.T., Lee, C.S. Application of WRF 3DVAR to operational typhoon prediction in Taiwan: Impact of outer loop and partial cycling approaches. *Wea. Forecasting* **2012**, 27, 1249–1263, doi:10.1175/WAF-D-11-00131.1.
4. Powers, J., Klemp, J., Skamarock, W., Davis, C., Dudhia, J., Gill, D., Coen, J., Gochis, D., Ahmadov, R., Peckham, S., Grell, G., Michalakes, J., Trahan, S., Benjamin, S., Alexander, C., DiMego, G., Wang, W., Schwartz, C., Romine, G., Liu, Z., Snyder, C., Chen, F., Barlage, M., Yu, W., Duda, M. The weather research and forecasting (WRF) model: overview, system efforts, and future directions. *Bull. Am. Meteorol. Soc.* **2017**, http://dx.doi.org/10.1175/BAMS-D-15-00308.1

5. Lakshmi, D., Murty, P.L.N., Bhaskaran, P.K., Sahoo, B., Srinivasa Kumar, T., Shenoi, S.S.C., Srikanth, A.S. Performance of WRF-ARW winds on computed storm surge using hydrodynamic model for Phailin and Hudhud cyclones. *Ocean. Eng.* **2017**, 131, 135–148.
6. Mattocks C., Forbes C. A real-time, event-triggered storm surge forecasting system for the state of North Carolina. *Ocean. Model.* **2008**, 25:95–119.
7. Lin, N., Emanuel, K.A. Grey swan tropical cyclones. *Nat. Climate Change* **2016**, 6, 106–111, doi:10.1038/nclimate2777.
8. Orton, P. M., Hall, T.M., Talke, S.A., Blumberg, A.F., Georgas, N., Vinogradov, S. A validated tropical-extratropical flood hazard assessment for New York harbor. *J. Geophys. Res. Oceans* **2016**, 121, 8904–8929, https://doi.org/10.1002/2016JC011679.
9. Krien, Y., Testut, L., Durand, F., Mayet, C., Islam A.K.M.S., Tazkia, A.R., Becker, M., Calmant, S., Papa, F., Ballu, V., Shum, C.K., Khan, Z.H. Towards improved storm surge models in the northern Bay of Bengal. *Continental Shelf Research* **2017**, 135, 58-73.
10. Shao, Z., Liang, B., Li, H., Wu, G., Wu, Z. Blended wind fields for wave modeling of tropical cyclones in the South China Sea and East China Sea. *Applied Ocean Research* **2018**, 71, 20-33.
11. Feng, X., Li, M., Yin, B., Yang, D., Yang, H. Study of storm surge trends in typhoon-prone coastal areas based on observations and surge-wave coupled simulations. *Int. J. Appl. Earth Obs. Geoinf.* **2018**, https://doi.org/10.1016/j.jag.2018.01.006.
12. Tan, C., Fang, W. Mapping the Wind Hazard of Global Tropical Cyclones with Parametric Wind Field Models by Considering the Effect of Local Factors. *Int. J. Disaster Risk Sci.* **2018**, https://doi.org/10.1007/s13753-018-0161-1.
13. Niedoroda, A. W., Resio, D. T., Toro, G. R., Divoky, D., Das, H. S., and Reed, C. W. Analysis of the coastal Mississippi storm surge hazard, *Ocean Eng.* **2010**, 37, 82–90.
14. Haigh, I. D., MacPherson, L. R., Mason, M. S.,Wijeratne, E. M. S., Pattiaratchi, C. B., Crompton, R. P., and George, S. Estimating present day extreme water level exceedance probabilities around the coastline of Australia: tropical cyclone-induced storm surges, *Clim. Dynam.* **2014**, 42, 139–157.
15. Krien, Y., Dudon, B., Roger, J., Zahibo, N. Probabilistic hurricane-induced storm surge hazard assessment in Guadeloupe, Lesser Antilles. *Nat. Haz. Earth Syst. Sci.* **2015**, 15, 1711-1720.
16. Krien, Y., Dudon, B., Roger, J., Arnaud, G., Zahibo, N. Assessing storm surge hazard and impact of sea level rise in Lesser Antilles-Case study of Martinique. *Nat. Haz. Earth Syst. Sci.* **2017**, 17, 1559-1571.
17. Lin, N., Chavas, D. On hurricane parametric wind and applications in storm surge modeling. *J. Geophys. Res.* **2012**, 117, D09120. http://dx.doi.org/10.1029/2011JD017126.
18. Olfateh, M., Callaghan, D.P., Nielsen, P., Baldock, T.E. Tropical cyclone wind field asymmetry—development and evaluation of a new parametric model, *J. Geophys. Res. Oceans* **2017**, 122, 458–469.
19. Knaff, J.A., S.P. Longmore, R.T. DeMaria, Molenar, D.A. Improved Tropical-Cyclone Flight-Level Wind Estimates Using Routine Infrared Satellite Reconnaissance. *J. Appl. Meteor. Climatol*. **2015**, 54, 463-478.
20. Dolling, K., E. Ritchie, Tyo, J. The Use of the Deviation Angle Variance Technique on Geostationary Satellite Imagery to Estimate Tropical Cyclone Size Parameters. *Wea. Forecasting* **2016**, 31, 1625–1642, doi: 10.1175/WAF-D-16-0056.1.
21. Mueller, K. J., DeMaria, M., Knaff, J.A., Kossin, J.P., Vonder Haar, T.H. Objective estimation of tropical cyclone wind structure from infrared satellite data. *Wea. Forecasting* **2006**, 21, 990–1005, doi:10.1175/WAF955.1.
22. Figa-Saldana, J., Wilson, J.J.W., Attema, E., Gelsthorpe, R., Drinkwater, M.R., Stoffelen, A. The advanced scatterometer (ASCAT) on the meteorological operational (MetOp) platform: A follow on for European wind scatterometers. *Canadian Journal of Remote Sensing* **2002**, 28, 404-412.
23. Madsen, N. M., Long, D.G. Calibration and Validation of the RapidScat Scatterometer Using Tropical Rainforests. *IEEE Trans. Geosci. Remote Sens.* **2016**, 54, 2846-2854.
24. Meissner, T., Wentz, F.J. Wind vector retrievals under rain with passive satellite microwave radiometers, *IEEE Trans. Geosci. Remote Sens*. **2009**, 47, 3065–3083, doi:10.1109/TGRS.2009.2027012
25. El-Nimri, S. F., Lindwood Jones, W., Uhlhorn, E., Ruf, C., Johnson, J., Black, P. An improved C-band ocean surface emissivity model at hurricane-force wind speeds over a wide range of Earth incidence angles, *IEEE Geosci. Remote Sens. Lett*. **2010**, 7, 641–645, doi:10.1109/LGRS.2010.2043814.

26. Reul N., Tenerelli J., Chapron B., Vandemark D., Quilfen Y., Kerr, Y. SMOS satellite L-band radiometer: A new capability for ocean surface remote sensing in hurricanes. *Journal of Geophysical Research* **2012**, vol. 117, C02006, doi: 10.1029/2011JC007474.
27. Reul N., Chapron B., Zabolotskikh E., Donion C., Mouche A.A., Tenerelli J., Collard F., Piolle J.F., Fore A., Yueh S., Cotton J., Francis P., Quilfen Y., Kudryavtsev V. A new generation of tropical cyclone size measurements from space. *Bull. Am. Meteorol. Soc.* **2017**, 98: 2367–2385, https://doi.org/10.1175/BAMS-D15-00291.1.
28. Zabolotskikh E., Mitnik L. M., Reul N., Chapron B. New Possibilities for Geophysical Parameter Retrievals Opened by GCOM-W1 AMSR2. *IEEE Journal of Selected Topics in Applied Earth Observations and Remote Sensing* **2015**, PP(99), 1-14. Publisher's official version : http://dx.doi.org/10.1109/JSTARS.2015.241651.
29. Fore, A. G., Yueh, S.H., Tang, W., Stiles, B., Hayashi, A.K. Combined Active/Passive Retrievals of Ocean Vector Wind and Sea Surface Salinity With SMAP. *IEEE Trans. Geosci. Remote Sens.* **2016**, 54(12), 7396-7404.
30. Foti, G., Gommenginger, C., Jales, P., Unwin, M., Shaw, A., Robertson, C., Rosell, J. Spaceborne GNSS reflectometry for ocean winds: First results from the UK TechDemoSat-1 mission. *Geophys. Res.Lett.* 2015, vol. 42, no. 13, pp. 5435–5441. http://dx.doi.org/10.1002/2015GL064204
31. Ruf, C., and Coauthors. New Ocean Winds Satellite Mission to Probe Hurricanes and Tropical Convection. *Bull. Amer. Meteor. Soc.* **2016**, 97, 385-395, doi:10.1175/BAMS-D-14-00218.1.
32. Morris, M., Ruf, C. Determining Tropical Cyclone Surface Wind Speed Structure and Intensity with the CYGNSS Satellite Constellation. *J. Appl. Meteor. Climatol*. **2017**, doi:10.1175/JAMC-D-16-0375.1
33. Holland, G. An Analytic Model of the Wind and Pressure Profiles in Hurricanes. *Monthly Weather Review* **1980**, 108:1212–1218.
34. Willoughby, H.E., Rahn, M.E. Parametric representation of the primary hurricane vortex. Part I: Observations and evaluation of the Holland (1980) model. *Mon. Wea. Rev*. **2004**, 132, 3033–3048.
35. Jelesnianski, C.P., Taylor, A.D. A preliminary view of storm surges before and after storm modifications. *NOAA Technical Memorandum. ERL WMPO-3, National Oceanic and Atmospheric Administration, U.S. Department of Commerce* **1973**, pp.33.
36. Emanuel, K., Rotunno, R. Self-stratification of tropical cyclone outflow, Part I: Implications for storm structure, *J. Atmos. Sci*. **2011**, 68, 2236–2249.
37. Murty, P.L.N., Bhaskaran, P.K., Gayathri, R., Sahoo, B., Srinivasa Kumar, T., SubbaReddy, B. Numerical study of coastal hydrodynamics using a coupled model for Hudhud cyclone in the Bay of Bengal, *Estuarine, Coastal and Shelf Science* **2016**, doi: 10.1016/j.ecss.2016.10.013.
38. Powell, M. D., Vickery, P.J., Reinhold, T.A. Reduced drag coefficient for high wind speeds in tropical cyclones, *Nature* **2003**, 422(6929), 279–283, doi:10.1038/nature01481.
39. Willoughby, H. E., Rahn, M. E., Darling, R. W. R. Parametric representation of the primary hurricane vortex. Part II: A new family of sectionally continuous profiles. *Mon. Weath. Rev.* **2006**, 134, 1102–1120.
40. Saïd, F., Katzberg, S.J., Soisuvarn, S. Retrieving Hurricane Maximum Winds Using Simulated CYGNSS Power-Versus-Delay Waveforms. *IEEE Journal of Selected Topics in Applied Earth Observations and Remote Sensing* **2017**. DOI:10.1109/JSTARS.2017.2695878
41. ASCAT Wind Product User Manual, KNMI, De Bit, The Netherlands, **2013**. [Online]. Available: http://projects.knmi.nl/ scatterometer/publications/pdf/ASCAT_Product_Manual.pdf
42. Verhoef, A., Portabella, M., and Stoffelen, A. High-resolution ASCAT scatterometer winds near the coast. *IEEE Trans. Geosci. Remote Sens*. **2012**, vol. 50, no. 7, pp. 2481–2487, doi:10.1109/TGRS.2016.2544835
43. Hu, K., Chen, Q., Kimball, S.K. Consistency in hurricane surface wind forecasting : an improved parametric model. *Nat. Hazards* **2012**, 61, 1029-1050.
44. Emanuel, K. *Tropical cyclone energetics and structure*, in Atmospheric Turbulence and Mesoscale Meteorology, edited by E. Fedorovich, R. Rotunno, and B. Stevens **2004**, pp. 165–192, Cambridge Univ. Press, Cambridge, U. K., doi:10.1017/CBO9780511735035.010.
45. Jelesnianski, C. P., Chen, J., Shaffer, W.A. *SLOSH: Sea, lake, and overland surges from hurricanes, NOAA Tech. Rep.* **1992** NWS 48, NOAA AOML Library, Miami, Fla.
46. Brennan, M.J, Hennon, C.C., Knabb, R.D. The Operational Use of QuikSCAT Ocean Surface Vector Winds at the National Hurricane Center. *Weather and Forecasting* **2009**, 24, 621-645.
47. Chavas, D. R., Lin, N., Emanuel, K. A model for the complete radial structure of the tropical cyclone wind field. Part I: Comparison with observed structure. *J. Atmos. Sci.* **2015**, 72, 3647–3662, doi:https://doi.org/10.1175/JAS-D-15-0014.1

528 48. Zhang, Y., Ye, F., Stanev, E.V., Grashorn, S. Seamless cross-scale modeling with SCHISM. *Ocean Modelling*
529 **2016**, 102, 64–81.
530 49. Carrère, L., Lyar, F., Cancet, M., Guillot, A., Roblou, L. FES2012: A new global tidal model taking
531 advantage of nearly 20 years of altimetry. In: *Paper presented at Proceedings of The Symposium 20 Years of*
532 *Progress in Radar Altimetry*, **2012**, Venice.
533 50. Saha, S., et al. *NCEP Climate Forecast System Version 2 (CFSv2) Monthly Products*. Research Data Archive at
534 the National Center for Atmospheric Research, Computational and Information Systems Laboratory, **2012**,
535 https://doi.org/10.5065/D69021ZF. Accessed 27/10/2017.
536 51. Pineau-Guillou, L., Ardhuin, F., Bouin, M.N., Redelsperger, J.L., Chapron, B., Bidlot, J.R., Quilfen, Y.
537 Strong winds in a coupled wave-atmosphere model during a North Atlantic storm event: evaluation
538 against observations. *Q. J. R. Meteorol. Soc.* **2017**, DOI:10.1002/qj.3205.